Enhanced particle fluxes and heterotrophic bacterial activities in Gulf of Mexico bottom waters following storm-induced sediment resuspension

Ziervogel K.[a,*], Dike C.[b], Asper V.[b], Montoya J.[c], Battles J.[d], D'souza N.[e], Passow U.[f], Diercks A.[g], Esch M.[d,1], Joye S.[d], Dewald C.[h], Arnosti C.[a]

[a] University of North Carolina at Chapel Hill, Department of Marine Sciences, Venable Hall, CB 3300, Chapel Hill, NC 27599-3300, USA
[b] University of Southern Mississippi, Department of Marine Sciences, Stennis Space Center, MS 395259, USA
[c] Georgia Institute of Technology, School of Earth and Atmospheric Sciences, Atlanta, GA 30332-0340, USA
[d] University of Georgia, Department of Marine Sciences, Rm 220 MARS Building, Athens, GA 30602-3636, USA
[e] Lamont-Doherty Earth Observatory, Columbia University, Palisades, NY 10964, USA
[f] University of California Santa Barbara, Marine Science Institute, Santa Barbara, CA 93106, USA
[g] University of Southern Mississippi, Department of Marine Sciences, Hattiesburg, MS 39406, USA
[h] Friedrich Schiller University Jena, Otto Schott Institute of Materials Research, D-07743 Jena, Germany

ARTICLE INFO

Available online 19 June 2015

Keywords:
Bottom nepheloid layer (BNL)
Resuspension
Microbial enzymatic activities
Bacterial productivity
Bacterial cell counts
Water column
Mississippi Canyon

ABSTRACT

Bottom nepheloid layers (BNLs) in the deep sea transport and remobilize considerable amounts of particulate matter, enhancing microbial cycling of organic matter in cold, deep water environments. We measured bacterial abundance, bacterial protein production, and activities of hydrolytic enzymes within and above a BNL that formed in the deep Mississippi Canyon, northern Gulf of Mexico, shortly after Hurricane Isaac had passed over the study area in late August 2012. The BNL was detected via beam attenuation in CTD casts over an area of at least 3.5 km^2, extending up to 200 m above the seafloor at a water depth of ~1500 m. A large fraction of the suspended matter in the BNL consisted of resuspended sediments, as indicated by high levels of lithogenic material collected in near-bottom sediment traps shortly before the start of our sampling campaign. Observations of suspended particle abundance and sizes throughout the water column, using a combined camera-CTD system (marine snow camera, MSC), revealed the presence of macroaggregates (> 1 mm in diameter) within the BNL, indicating resuspension of canyon sediments. A distinct bacterial response to enhanced particle concentrations within the BNL was evident from the observation that the highest enzymatic activities (peptidase, β-glucosidase) and protein production (^{3}H-leucine incorporation) were found within the most particle rich sections of the BNL. To investigate the effects of enhanced particle concentrations on bacterial activities in deep BNLs more directly, we conducted laboratory experiments with roller bottles filled with bottom water and amended with experimentally resuspended sediments from the study area. Macroaggregates formed within 1 day from resuspended sediments; by day 4 of the incubation bacterial cell numbers in treatments with resuspended sediments were more than twice as high as in those lacking sediment suspensions. Cell-specific enzymatic activities were also generally higher in the sediment-amended compared to the unamended treatments. The broader range and higher activities of polysaccharide hydrolases in the presence of resuspended sediments compared to the unamended water reflected enzymatic capabilities typical for benthic bacteria. Our data suggest that the formation of BNLs in the deep Gulf of Mexico can lead to transport of sedimentary organic matter into bottom waters, stimulating bacterial food web interactions. Such storm-induced resuspension may represent a possible mechanism for the redistribution of sedimented oil-fallout from the Deepwater Horizon spill in 2010.

1. Introduction

Particulate organic matter derived from the photic zone provides nutrients and energy for deep ocean microbial food webs and higher trophic levels (Aristegui et al., 2009). Major pathways for organic matter export to the deep sea include downward flux

* Corresponding author. Tel.: +1 919 8432464.
E-mail address: ziervoge@email.unc.edu (K. Ziervogel).
[1] Present address: University of North Carolina at Chapel Hill, Department of Marine Sciences, Venable Hall, CB 3300, Chapel Hill, NC 27599-3300, USA.

http://dx.doi.org/10.1016/j.dsr2.2015.06.017

of marine snow and feces, as well as near-bed lateral transport of particulate matter along continental slopes (Thomsen, 1999). Particle advection above the seafloor is driven by bottom flow and seafloor topography, affecting particle and elemental fluxes on spatial scales from a few centimeters to meters above the deep seafloor (Graf and Rosenberg, 1997). Larger scale transport of particulate matter along continental slopes is triggered by gravity flow of fine-grained shelf sediment suspensions, forming deep-sea turbidity currents or by storm activity (Hollister and McCave, 1984). Hydrodynamic forces resulting from storms affecting the surface ocean propagates to the deep ocean, leading to resuspension of deep-sea sediments and formation of bottom water turbidity layers, also known as bottom nepheloid layers (BNLs; McCave, 1986).

Deep-sea BNLs can form on a seasonal basis, as seen in the deep northwestern Mediterranean Sea during winter, when particle-rich shelf waters trigger downslope turbidity currents and resuspension of slope sediments (Puig et al., 2013). Storm-induced perturbations of the surface ocean can also result in resuspension of the seabed, as periodically observed in the Eel River submarine canyon of the northern California margin (Puig et al., 2004). The Mississippi Canyon, an undersea canyon in the northern Gulf of Mexico south of Louisiana, is also frequently affected by high flow events of down-canyon turbidity currents and sediment resuspension in the aftermath of passing storms (Ross et al., 2009).

The vast majority of studies on deep ocean BNLs have focused on measuring and modeling associated hydrodynamic conditions (Fohrmann et al., 1998). Information on bacterial transformation of organic matter within BNLs are comparatively rare and limited to a few oceanic regions, despite their important role in processing and transforming organic matter associated with suspended particles near the deep seafloor (Turley, 2000). In the deep Arabian Sea, elevated heterotrophic bacterial abundance, protein production, and organic matter degradation have been reported in particle-rich bottom waters (Boetius et al., 2000). Investigations in bottom waters of the Mid-Atlantic Ridge revealed substantial bacterial activities and organic matter degradation rates associated with suspended particles (Baltar et al., 2010). Substantial bacterial biomass associated with (re-) suspended sediments was also found above continental slope sediments of the Norwegian Sea (Thomsen and Graf, 1994) and the northeastern shelf of Greenland (Ritzrau et al., 1997). Ritzrau et al. (1997) also reported high levels of bacterial activities, as indicated by elevated rates of amino acid uptake in aggregates of resuspended sediments in these high latitude systems. In shallow coastal environments, sediment resuspension enhances the upward flux of sediment-associated benthic bacteria (Stevens et al., 2005), often resulting in increased rates and activities of bacterial hydrolytic enzymes in the overlying water (Chrost and Rieman, 1994; Ritzrau and Graf, 1992; Ziervogel and Arnosti, 2009).

To investigate the effects of enhanced particle fluxes on rates and activities of deep ocean heterotrophic bacteria, we measured bacterial abundance, protein production and hydrolytic enzyme activities within a BNL that formed in the deep Mississippi Canyon shortly after Hurricane Isaac made landfall on the Louisiana coast in late August 2012. We also measured bottom water bacterial dynamics during a laboratory experiment, mimicking particle interactions and transport of resuspended sediments from the study area.

2. Material and methods

2.1. Study site

Our study site is located in the Mississippi Canyon, northern Gulf of Mexico, approximately 80 km to the southeast of the Mississippi River mouth (Fig. 1). The water column survey (CTD profiles, in situ aggregate profiles, water column samples; see Sections 2.2 and 2.3) near Oceanus site 26 (OC26; 28° 44.20'N, 88° 23.23'W; water depth: 1500 m) was conducted from September 05 2012 to September 13, 2012, onboard the R/V *Endeavor*. OC26 is located 3.5 km to the south of the sunken Deepwater Horizon (DWH) oil rig and the Macondo wellhead (Fig. 1) that exploded in April 2010, causing the largest oil spill of the offshore oil and gas industry to date (Atlas and Hazen, 2011). Our water sampling campaign at OC26 started one week after Hurricane Isaac made landfall on the Louisiana coast near the Mississippi River mouth on August 28, 2012. The slow moving hurricane produced sustained tropical force winds for up to 45 h in coastal areas and heavy rainfall. A vast amount of water was pushed westward against the southeastern shoreline of Louisiana, causing the Mississippi River to flow upstream for 24 h, with the storm surge advancing > 300 river miles (Berg, 2013).

Sediment cores for the roller bottle experiments with resuspended sediments (see Section 2.5) were collected onboard the R/V *Falkor* in November 2012 at OC26 as well as 5 km to the

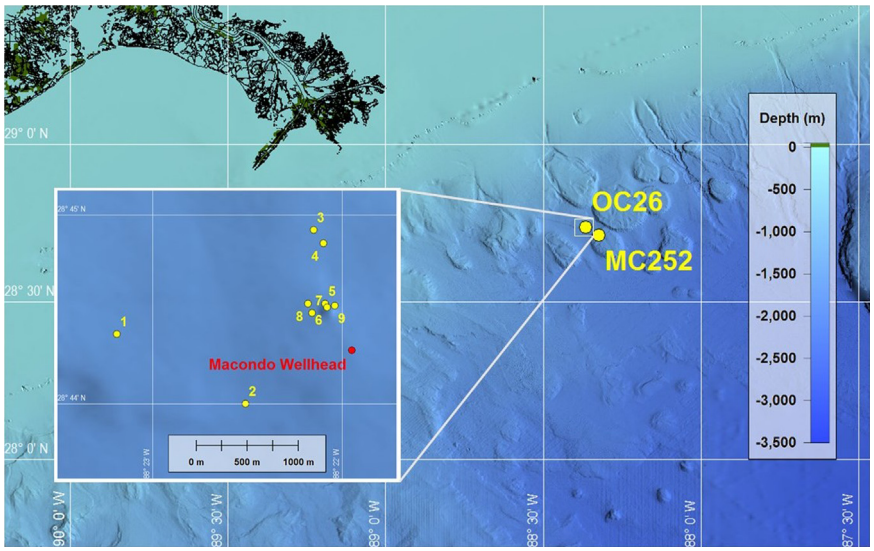

Fig. 1. Map of the sampling sites in the Oceanus Site 26 (OC26) area. Numbers in the insert correspond to cast numbers from Table 1.

south-east at Mississippi Canyon Site 252 (MC252: 28° 42.73'N, 88° 19.45'W; water depth: 1500 m; Fig. 1).

2.2. Water column sampling

Water column profiles of light attenuation (turbidity) were measured using a 25 cm transmissometer (WET Labs C-Star 25 cm) attached to a conductivity-temperature-depth (CTD) rosette (Sea-Bird Electronics). Six CTD profiles were obtained over the course of 8 days (see Table 1 for locations and dates of the casts). Three of the casts (5, 7, 8) were clustered within an area of approximately 0.5 km. Cast 1 was 3.5 km to the west, cast 2 was 2.5 km to the southwest, and cast 4 was 1.5 km to the north of this cluster (Fig. 1). Water samples for analysis of bacterial abundance and activities (see Section 2.6) were taken at specific depths during CTD casts 1, 2, and 7 using Niskin bottles attached to the CTD rosette.

2.3. In situ particle observations

Three water column profiles of suspended particles were obtained using a combined camera-CTD system (marine snow camera, MSC) mounted on an aluminum frame (Table 1). MSC cast 3 was located close to CTD cast 4, to the north of the cluster of CTD casts 5, 7, and 8 (Fig. 1). MSC casts 6 and 9 were located within the cluster itself. The MSC takes 1 image every 10 s while the system is being lowered at 10 m min^{-1} resulting in an image approximately every 1.7 m. A collimated light source illuminated a defined volume of water allowing for volume specific calculations. The camera system is only deployed during night hours to avoid natural light interference with the imaged volume in the upper part of the water column.

The images were analyzed for particle abundance and sizes using Image-Pro software. Particles > 0.5 mm in diameter were counted, and grouped into 2 size classes: 0.5–1 mm in diameter (hereafter referred to as microaggregates), and > 1 mm in diameter (macroaggregates; note that most of the macroaggregates were 1–2 mm in diameter).

2.4. Sediment trap deployment

A time series sediment trap mooring (Kiel KUM) was deployed 100 m above the seafloor at OC26 from August 25, 2010, until October 19, 2011 (Deployment 1). Note that sediment trap samples prior to January 2011 were impacted by oil-fallout sedimentation from the DWH oil spill and therefore not considered for the analysis shown here. Two McLane timeseries sediment traps were deployed at 30 m and 120 m above the seafloor from June 28, 2012, until September 8, 2012 (Deployment 2) and then redeployed on September 12, 2012 until September 12, 2013 (Deployment 3; collection intervals for all three deployments: 17–21 days). Both types of funnel shaped traps have a 0.5 m^2 collection surface, which is covered with a hexagonal lattice grid baffle that reduces wash-out. Particles falling into the trap were fixed in situ with mercuric chloride (final concentration of ~0.14%) in a salinity gradient (40 PSU). Upon retrieval, the cups containing the fixed samples were stored and transported in the dark at 4 °C back to the University of California, Santa Barbara. Prior to analysis, the sampling cups were gently mixed and the samples were allowed to resettle for 5 days. The material was then split using a Foulsom or McLane splitter. Artificial seawater was used to rinse the sampling cups. Sample splits were analyzed for the parameters listed below (Section 2.6.4).

Table 1
Dates and locations of CTD and Marine Snow Camera (MSC) casts.

Cast #	Date	Lat (°N)	Long (°W)	Events (ID)
1	Sept 05, 2012	28 44.37	88 23.19	CTD profile (02.01)
2	Sep 11, 2012	28 44.00	88 22.51	CTD profile (10.04)
3	Sept 12, 2012	28 44.92	88 22.15	Marine Snow Camera (10.07)
4	Sept 12, 2012	28 44.85	88 22.10	CTD profile (10.09)
5	Sept 12, 2012	28 44.53	88 22.09	CTD profile (10.13)
6	Sept 13, 2012	28 44.51	88 22.08	Marine Snow Camera (10.15)
7	Sept 13, 2012	28 44.48	88 22.16	CTD profile (10.19)
8	Sept 13, 2013	28 44.53	88 22.18	CTD profile (10.21)
9	Sept 14, 2013	28 44.52	88 22.04	Marine Snow Camera (10.22)

2.5. Laboratory investigation of resuspended sediment

To complement field data, which represent a snapshot of particle inventories and bacterial activities at the time of sampling, we conducted a roller bottle experiment with bottom water containing resuspended sediments from the study area. Roller bottles mimic interactions and aggregate formation of suspended particulate matter, as the rotation of roller bottles prevents sedimentation of particles (Ziervogel et al., 2012). This experiment was designed to study interactions of resuspended sediments in OC26 bottom waters under laboratory conditions.

To obtain sufficient sedimentary particulate matter for the roller bottle incubations, we collected sediments from incubation experiments conducted aboard the R/V *Falkor*. Sediment cores containing overlying water were collected with a multicorer at OC26 and MC252. A Niskin bottle attached to the multicorer was used to collect additional bottom water. The sediment cores were moved to a cold room (4 °C) and incubated shortly after sampling. A stir bar (5 cm in length) connected to a piece of tubing and joined to the lid of the core was positioned 6–8 cm above the sediment-water interface. The water was mixed by placing a rotating magnet in the middle of 6 sediment cores. At the end of the experiment (3 days), water overlying the sediment cores that contained resuspended sediments was gently removed, stored at 4 °C, and transported cold on blue ice back to the University of North Carolina at Chapel Hill. The roller bottle incubations were initiated promptly after the overlying water reached the home laboratory, 9 days after the start of the onboard incubations.

Experimentally resuspended sediments in bottom water (hereafter referred to as BW+seds) were transferred into one 1-L Pyrex © glass bottle (total bottle volume: 1150 mL; sample volume: 1000 mL; particle concentration: 0.1 ppt v/v). The second 1 L glass bottle lacked sediments and was filled to the 1 L mark with bottom water (BW), which had been collected using the Niskin bottle mounted above the multicorer. A third bottle contained 0.1-μm filtered and autoclaved bottom water (BW control) acted as a killed control. Roller bottles were incubated on a roller table at 3.5 rpm for 7 days at 4 °C in the dark. Before the start of the roller bottle incubations (Day 0) and after 1 and 4 days, the bottle containing resuspended sediments was photographed and inspected for macroaggregate formation. Approximately 50 mL of bottle water was removed at days 0, 4 and 7 for bacterial activity analysis (see Section 2.6 for a detailed description of the analytical methods). Subsamples of BW+seds at days 4 and 7 contained fragile macroaggregates that were disrupted during sampling. The first incubation period (0–4 days) reflects approximate residence times of in situ bottom water macroaggregates before re-deposition (see Section 4).

2.6. Analysis

2.6.1. Bacterial cell counts

Up to 10 mL of water taken from the CTD at OC26 (field samples) and from the roller bottles (experimental samples) were fixed with formalin (2% final conc.) immediately after collection and stored in the dark at 4 °C. A known volume of each fixed sample was drawn through

a 25 mm, 0.2 μm pore, black polycarbonate filter (Millipore, type GTPB) using low vacuum. The filters were transferred to clean microscope slides. 10 μl of a freshly prepared staining solution containing 50% glycerol in 1 × PBS at pH 7.4, ascorbic acid (1% final conc. v/v), and SYBR green I stain (0.45% final conc. v/v) was placed in the middle of a cover slip (25 mm × 25 mm) and inverted onto the filter (Lunau et al., 2005). The slide was then placed in the dark at 4 °C, until the weight of the cover slip dispensed the stain evenly across the filter. Bacterial cells were counted with a Nikon Labophot-2 epifluorescence microscope with blue light excitation at 1000 × magnification. Bacterial cells in roller bottle water were stained with 4',6-diamidino-2-phenylindole (DAPI; Porter and Feig, 1980), and stored at −20 °C until enumeration under an epifluorescence microscope (Olympus, magnification x1000; UV excitation) equipped with a digital camera (Olympus TH4-100). In both cases (field and experimental samples) a minimum of 200 cells each filter were enumerated.

2.6.2. Bacterial leucine incorporation

Incorporation of the amino acid leucine is used to trace bacterial protein synthesis and thus biomass production in the ocean (Kirchman, 2001). Tritiated leucine was added at substrate saturating levels (field samples: 11.4 nM final conc.; experimental samples: 20 nM final conc.) to triplicate microcentrifuge tubes containing 1.5 mL to 1.7 mL of seawater. Killed controls contained substrate and 87 μL of 100% trichloroacetic acid (TCA). Incubations were conducted in the dark at in situ temperature for 1–2 h (field samples) and 4-5 h (experimental samples). Incubations were terminated by adding 87 μL of 100% TCA, followed by centrifugation of the tubes at 5000 g (experimental samples) and 10000 g (field samples) for 10 − 15 min using a FlexiFuge Centrifuge (Argos). Pellets were consecutively washed with 5% ice-cold TCA and 80% ice-cold ethanol and air dried. The radioactivity of the samples, which reflected incorporation of tracer into biomass, was measured in a scintillation counter.

2.6.3. Hydrolytic enzyme activities

Hydrolytic enzymes are the major means for heterotrophic bacteria to access and degrade high molecular weight organic matter in the ocean (Arnosti, 2011). Enzyme activities were measured using L-leucine-4-methylcoumarinyl-7-amide (MCA) hydrochloride and 4-methylumbelliferone (MUF) β-D-glucopyranoside (Sigma-Aldrich) as substrate proxies for leucine-aminopeptidase (hereafter referred to as peptidase) and β-glucosidase activities, respectively (Hoppe, 1983). Enzymatic hydrolysis of MCA- and MUF-substrate proxies can be measured with short-term (several hour) incubations, and is generally considered to reflect activities of the in situ microbial community. Three mL of seawater were added to replicate disposable methacrylate cuvettes containing a single substrate at saturation levels (final concentration: 300 μM). Cuvettes were incubated in the dark at in situ temperature; fluorescence was measured immediately after sample addition and in subsamples from the incubation cuvette at two additional times over the course of 24 h. Fluorescence was measured by adding 1 ml sample to 1 ml 20 mM borate buffer (pH 9.2) using a Turner Biosystems TBS-380 fluorometer (excitation/emission channels set to "UV"; 365 nm excitation, 440–470 nm emission). Fluorescence changes were calibrated using MUF and MCA standard solutions in seawater, and used to calculate hydrolysis rates. Killed controls (autoclaved seawater) showed only minor changes in fluorescence over time.

Following the roller bottle incubation, we investigated the capabilities of the microbial community to access and degrade a range of structurally distinct polysaccharides. Polysaccharide hydrolysis experiments were conducted using fluorescently-labeled (FLA) pullulan, laminarin, xylan, fucoidan, arabinogalactan, and chondroitin sulfate (polysaccharides obtained from Fluka or Sigma; see Arnosti (2003) for a description of the substrate labeling and the set-up of the hydrolysis experiments). This suite of polysaccharides differs in monomer composition and linkage position; many are components of marine algae (Painter, 1983), and are therefore present in considerable quantities in the ocean (Alderkamp et al., 2007). Enzymes that specifically hydrolyze these substrates have been identified in a variety of marine environments (Arnosti et al., 2011) including Mississippi Canyon bottom waters (Steen et al. 2012; Ziervogel and Arnosti, 2013).

Single FLA substrates were added to homogenized water from the three roller bottles at a final substrate concentration of 3.5 μM monomer equivalent. Roller bottle water was incubated in duplicate 15 ml glass vials in the dark at 4 °C for 22 days. Since the amount of time required for a polysaccharide pool to be hydrolyzed to lower molecular weights is not known *a priori*, incubations are conducted as time series. Thus 1 mL subsamples were taken after 0, 3, 7, 14, 22 days, filtered through 0.2 μm syringe filters and stored at −20 °C until analysis. Samples were analyzed using gel-permeation chromatography with fluorescence detection, as described in detail in Arnosti (2003). Substrates incubated with killed control waters showed no significant changes in molecular weights over time.

Polysaccharide degradation experiments require comparatively long incubation times and therefore integrate microbial enzymatic induction and growth responses (including possible changes in community composition) to substrate addition. We monitored the growth response of the microbial community to the addition of the polysaccharides over the time course of the incubation by measuring bacterial abundance (see Section 2.6.1) and ^{3}H-leucine incorporation rates (see Section 2.6.2) in each of the incubation vials, and in one glass vial without added polysaccharides.

Hydrolysis rates reported here represent potential rates, since added substrates (either substrate proxies or polysaccharides) compete with naturally-occurring substrates for enzyme active sites. Given the concentration of added substrate, however, hydrolysis rates are likely zero-order with respect to substrate and represent maximum potential rates.

2.6.4. Particulate organic and inorganic matter

Water collected from selected depths during the R/V *Endeavor* cruise were vacuum filtered onto replicate, pre-combusted GF/F filters (total filtered volume: 1000 mL) for particulate organic carbon (POC) analysis. The filters were acidified with 12 M HCl for 12 h to remove inorganic carbon prior to flash combustion to CO_2 and N_2 on a Carlo-Erba 1500 Elemental Analyzer, using acetanilide as a standard.

Quadruplicates of the sediment traps sample splits (between 1/25th and 1/2500th depending on the total amount of settled material; usually 1/500th) were filtered onto pre-weighed and pre-combusted (450 °C for 4–6 h) GF/F filters, briefly rinsed with Milli-Q water and dried at 60 °C before reweighing for dry weight (dw) analysis. Subsequently, replicate filters were combusted at 450 °C for 4–6 h to remove organic matter and reweighed again. POM was calculated as the difference between the total dry weight and the weight of the inorganic matter (PIM) remaining on the filter after combustion. Particulate inorganic carbon (PIC) was determined as the difference of the acidified (fumed with 10% HCl) and non-acidified particulate carbon, analyzed in duplicates using a CHN elemental analyzer (model CEC 44OHA by Control Equipment; now Exeter Analytical) following Shipe and Brzezinski (2003). Subsamples of the splits were filtered onto 0.6 μm polycarbonate filters for biogenic silica (BSi) analysis (DeMaster, 1981, Mortlock and Froelich 1989). The filters were hydrolyzed with Na_2CO_3 running a 5 h timeseries and analyzed colorimetrically. The

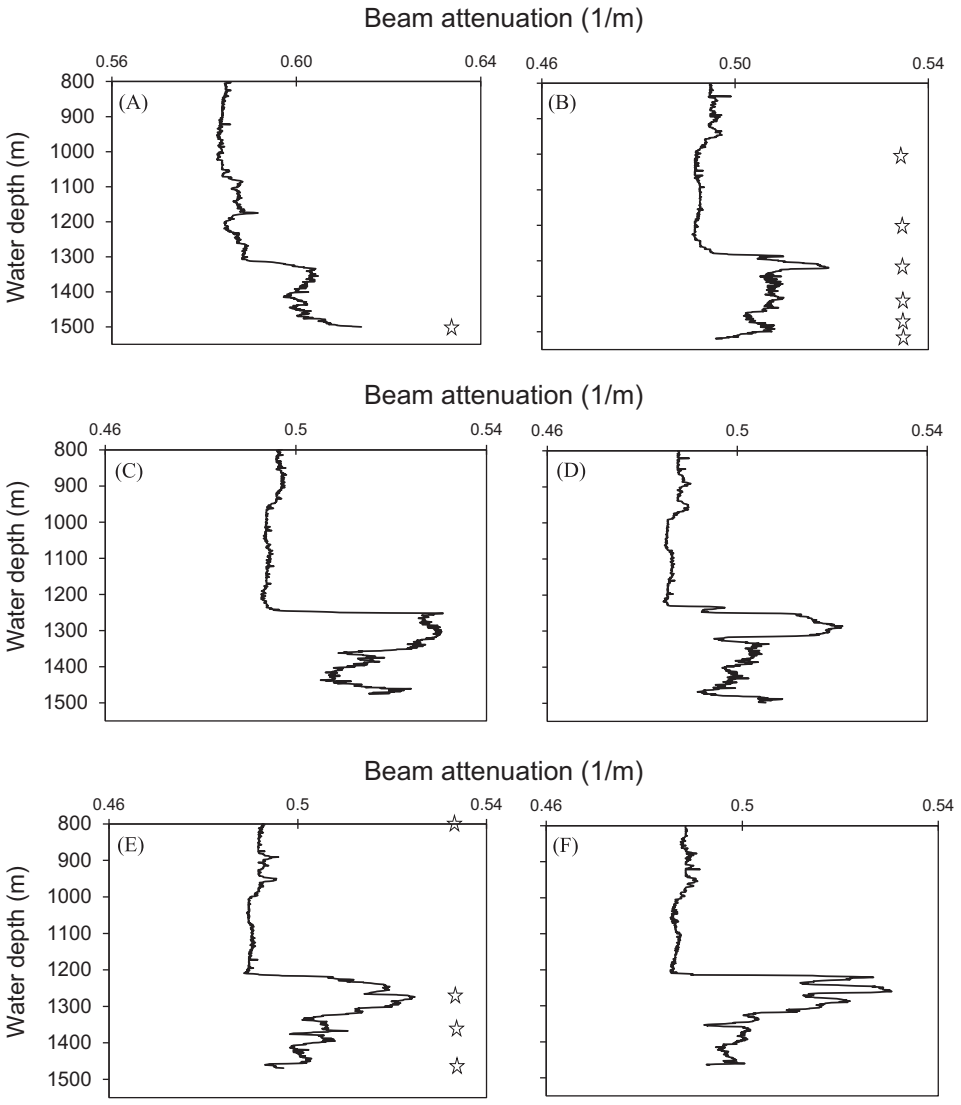

Fig. 2. Bottom water profiles of beam attenuation showing the bottom nepheloid layer (BNL) in all six CTD casts. The stars in A (cast 1), B (cast 2), and E (cast 7) indicate the water depths in which bacterial parameters were measured.

concentration of lithogenic material was calculated by subtracting PIC and BSi from PIM.

2.7. Statistical analysis

One-way ANOVAs at the 5% significance level were performed to test whether average rates of bottom water hydrolytic enzyme activities and leucine incorporation differ per depth (field samples) and time during the course of the roller bottle experiment (experimental samples). Post-hoc comparisons were made for all pairs using Scheffé's method. Enzyme activities and leucine incorporation rates during the 7-day roller bottle experiment were compared with Student's *t*-test at the 5% significance level.

3. Results

3.1. Field observations

3.1.1. Bottom nepheloid layer (BNL) at OC26

The six CTD profiles showed increased beam attenuation at around 250 m above the seafloor, indicating the presence of a thick bottom nepheloid layer (BNL) (Fig. 2; see Suppl. Fig. S1 for other parameters recorded with the shipboard CTD). All profiles had a distinct turbidity front in the uppermost part of the BNL. The thickness of the front was 100–120 m in cast 4 (Fig. 2C) as well as in the three clustered casts 5, 7, and 8 (Fig. 2D and F). The fronts were characterized by a sharp transition between the BNL and the overlying water column that was most pronounced in cast 4 (Fig. 2C). The remaining two casts to the southwest (cast 2) and west (cast 1) of the clustered location of casts 4, 5, 7, and 8 had a less pronounced turbidity transition (cast 1; Fig. 2A) and turbidity front (~60 m in cast 2; Fig. 2B).

3.1.2. In situ aggregate numbers and sizes

The three MSC casts showed a uniform distribution of total aggregate abundance in the uppermost 1200 m of the water column (~20 aggregates L^{-1}; Fig. 3; see also Suppl. Figs. S2 and S3 for beam attenuation profiles and aggregate pictures, respectively, recorded with the MSC). Aggregate abundance sharply increased in the BNL, reaching peak levels within the turbidity front of ~130 aggregates L^{-1} (cast 3; Fig. 3A), ~250 aggregates L^{-1} (cast 6; Fig. 3B), and ~200 aggregates L^{-1} (cast 9; Fig. 3C). Most of the aggregates were in the smaller size range (0.5–1 mm in diameter); however in cast 3, macroaggregates > 1 mm in diameter increased in relative

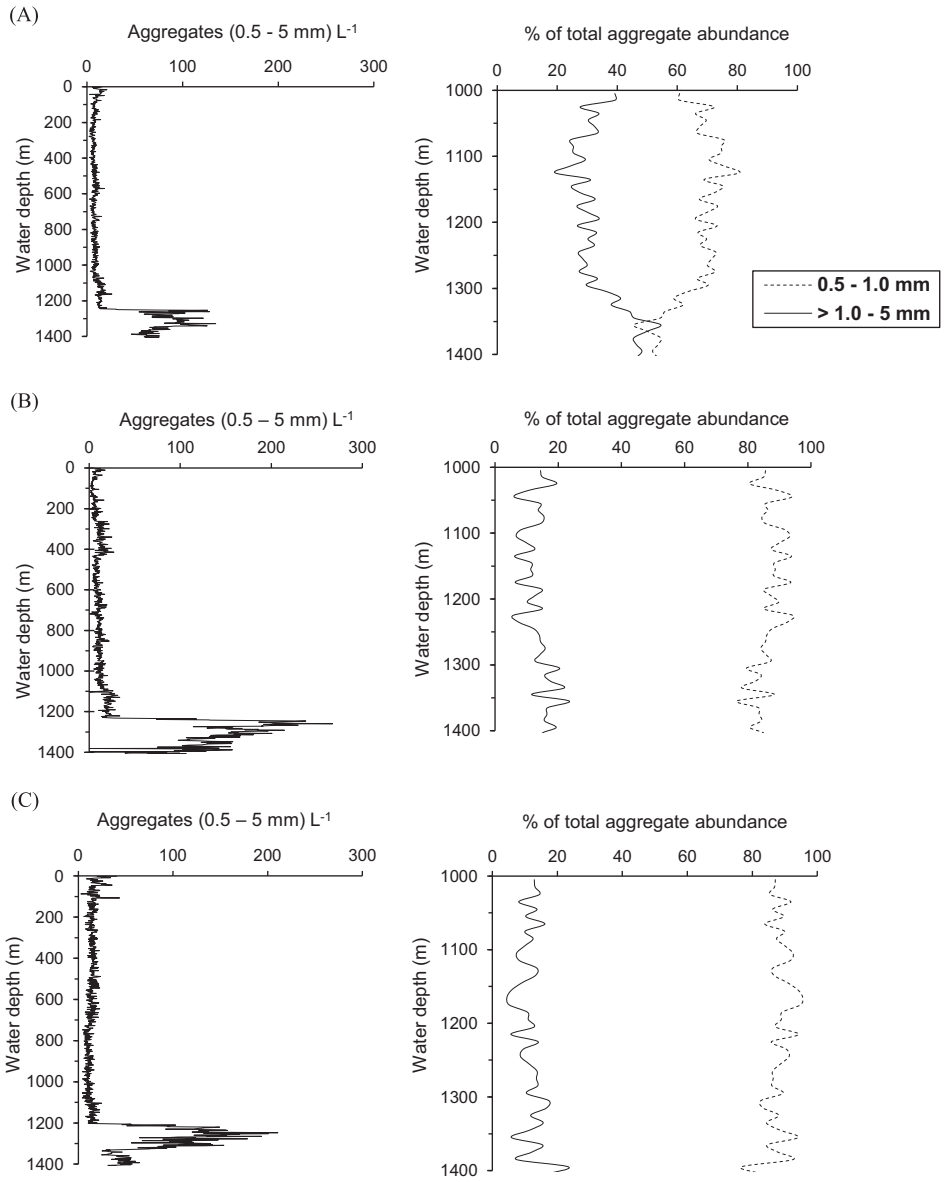

Fig. 3. Marine snow camera (MSC) casts. Water column profiles of total aggregates per liter on the left. Relative abundance (% of total aggregate numbers) of microaggregates (0.5–1 mm in diameter) and macroaggregates (> 1–5 mm) in bottom waters on the right.

abundance below the turbidity front, constituting 40% to 50% of the total numbers of aggregates near the seafloor (Fig. 3A).

3.1.3. *Bacterial activities and abundances at OC26*

Peptidase activities within the BNL were up to a factor of 3 higher on a volume basis compared to the overlying water (casts 2 and 7; Table 2). Lower peptidase activities in near-bottom waters compared to the mid-depth and surface water sample were only found in cast 1, where the BNL was less pronounced (Fig. 2). Highest peptidase activities near the seafloor were found at 1369 m in cast 7, well below the turbidity front. Cell-specific peptide hydrolysis rates at 1369 m in cast 7 also exceeded the other bottom water rates (Table 2, Fig. 4A) as well as those from the overlying water column by up to a factor 3.

Activities of β-glucosidase on a volume basis followed patterns very similar to peptidase activities, with higher rates within the BNL and lower rates above the BNL (casts 2 and 7). Cell-specific β-glucosidase activities in the BNL were higher than (cast 2) and similar to (cast 7) cell-specific rates of the overlying water (Fig. 4B). Bottom water rates in cast 1 were lower compared to the overlying water column of the same cast, as well as bottom waters in casts 2 and 7 (Table 2, Fig. 4B).

Near-bottom leucine incorporation rates in cast 2 were in the same range (at 1429 m) and only slightly higher (at 1479 and 1519 m) than bottom water rates in cast 1, and were substantially lower compared to those near the seafloor in cast 7 (Table 2, Fig. 4C). Highest bottom water rates in cast 2 were found within the turbidity front at 1320 m. Highest leucine incorporation rates were measured at 1369 m in cast 7.

For bacterial cells, overall highest bottom water abundances at 2.8×10^7 cells L^{-1} were found in cast 1 (Table 2). In cast 2, bacterial cell numbers in the BNL ranged between 0.7×10^7 cells L^{-1} (1320 m) and 1.2×10^7 cells L^{-1} (1479 m); slightly higher cell numbers at 1.5×10^7 cells L^{-1} were found below the turbidity front in cast 7.

3.1.4. *Particulate organic carbon at OC26*

Dry weight of particulate organic matter (POM) near the seafloor in cast 1 (1498 m) was in the same range as in the overlying water column at 285 m in the same cast. POM dry weight in cast 7 within the

Table 2
Water column profiles of bacterial cells (L^{-1}), peptidase and β-glucosidase activities (pM h^{-1}), leucine incorporation (pm h^{-1}), dry weight, and POC (μg L^{-1}) (average ± standard deviation except for bacterial cells). Cell-specific enzyme activities (amol $cell^{-1}$ h^{-1}) and leucine incorporation rates (amol $cell^{-1}$ day^{-1}) are in parenthesis. BNL samples are in bold; n.d. means not determined.

Cast #	Depth	Cells x 10^7	Peptidase	β−glucosidase	Leu incorp	Dry weight	POC	C/N
1	1	26.6	14690 ± 487 (55.3 ± 1.8)	1070 ± 67.2 (3.9 ± 0.2)	18.5 ± 4.3 (1.7 ± 0.4)	1000 ± 0	106.1 ± 11.9	10.6
	63	23.4	12761 ± 2202 (54.4 ± 9.4)	446 ± 85.9 (1.9 ± 0.4)	n.d.	1150 ± 50	103.6 ± 36.5	11.3
	285	2.1	890 ± 841 (41.6 ± 39.9)	71.1 ± 39.5 (3.3 ± 1.8)	1.5 ± 0.1 (1.7 ± 0.2)	850 ± 250	39.8 ± 27.2	9.5
	1498	**2.8**	**272 ± 31.5 (9.6 ± 1.1)**	**71.3 ± 36.3 (2.5 ± 1.3)**	**0.7 ± 0.0* (0.6 ± 0.0*)**	**1000 ± 100**	**36.5 ± 0.2**	**9.6**
2	300	2.6	1604 ± 26.3 (61.1 ± 1)	315 ± 62.5 (12 ± 2.4)	9.2 ± 0.8 (8.4 ± 0.7)	n.d.	n.d.	n.d.
	380	1.9	859 ± 7.2 (45.1 ± 0.4)	195 ± 2 (10.3 ± 0.1)	0.6 ± 0.3 (0.7 ± 0.4)	n.d.	n.d.	n.d.
	460	2	471 ± 124 (23.8 ± 6.2)	152 ± 17.0 (7.7 ± 0.9)	0.2 ± 0.1 (0.3 ± 0.1)	n.d	n.d	n.d
	600	1.7	394 ± 110 (22.7 ± 6.3)	155 ± 8.4 (8.9 ± 0.5)	2.2 ± 0.3 (3.1 ± 0.4)	n.d.	n.d.	n.d.
	800	1.3	745 ± 40.2 (59.6 ± 3.2)	139 ± 45.9 (11.1 ± 3.7)	0.6 ± 0.2 (1.2 ± 0.3)	n.d.	n.d.	n.d.
	1000	1	443 ± 117 (44.4 ± 17.2)	196 ± 39.8 (19.6 ± 4)	0.3 ± 0.1 (0.7 ± 0.2)	n.d.	n.d.	n.d.
	1200	**2.2**	**445 ± 42.7 (20.7 ± 2)**	**200 ± 10.6 (9.3 ± 0.5)**	**2.3 ± 0.1 (2.5 ± 0.1)**	**n.d.**	**n.d.**	**n.d.**
	1320	**0.7**	**452 ± 1.1 (60.7 ± 0.2)**	**201 ± 21.9 (27.1 ± 2.9)**	**3.7 ± 0.3 (11.8 ± 0.9)**	**n.d.**	**n.d.**	**n.d.**
	1429	**0.9**	**1161 ± 21.3 (131.9 ± 2.4)**	**248 ± 33 (28.1 ± 3.8)**	**0.2 ± 0.0* (0.4 ± 0.1)**	**n.d.**	**n.d.**	**n.d.**
	1479	**1.2**	**917 ± 31.0 (77.3 ± 2.6)**	**240 ± 30.7 (20.3 ± 2.6)**	**1.4 ± 0.4 (2.9 ± 0.9)**	**n.d.**	**n.d.**	**n.d.**
	1519	**0.9**	**1037 ± 47.5 (120 ± 5.5)**	**252 ± 108.5 (29.2 ± 12.5)**	**0.8 ± 0.1 (2.2 ± 0.9)**	**n.d.**	**n.d.**	**n.d.**
7	800	1.2	802 ± 38.2 (66.1 ± 3.1)	273.2 ± 6.1 (22.5 ± 0.5)	6 ± 0.3 (11.9 ± 0.6)	n.d.	n.d.	n.d.
	1287	**1**	**1009 ± 7.9 (102 ± 0.8)**	**241 ± 50.5 (24.5 ± 5.1)**	**2.3 ± 0.2 (5.5 ± 0.6)**	**2300 ± 900**	**27.5 ± 1.8**	**7.5**
	1369	**1.4**	**3060 ± 18.7 (214 ± 1.3)**	**408 ± 12.8 (28.5 ± 0.9)**	**209 ± 17.4 (350.7 ± 29.3)**	**n.d.**	**n.d.**	**n.d.**
	1459	**1.5**	**1227 ± 94.6 (82.5 ± 6.4)**	**213 ± 13.8 (14.3 ± 0.9)**	**5.6 ± 0.8 (9.1 ± 1.4)**	**n.d.**	**n.d.**	**n.d.**

* error < 0.05.

turbidity front at 1287 m was higher compared to the two depths in cast 1 (Table 2). The C/N ratio in the turbidity front in cast 7 was comparatively low (7.5 compared to 9.6 near the seafloor in cast 1).

3.1.5. Particulate matter in sediment traps

Composition of particulate matter collected at 120 m and 80 m above the seafloor during the final collection period of deployment 2 (August 12, 2012, to September 8, 2012) revealed an elevated contribution of lithogenic material (426 mg m^{-2} d^{-1}; Table 3) compared to other time periods, with a POM: dw ratio of 13%. During non-phytoplankton bloom conditions, sedimentation rates of lithogenic material were < 300 mg m^{-2} d^{-1} (median: 161; $n=30$) at a POM: dw ratio of 25%. Sedimentation events associated with the phytoplankton blooms that occasionally occurred throughout the deployment period (usually between March and June) were characterized by high sedimentation rates of POM (median 187 mg m^{-2} d^{-1}, $n=7$ vs. 58 mg m^{-2} d^{-1}, $n=30$) and lithogenic material (median: 494 mg m^{-2} d^{-1}, $n=7$) as sinking POM scavenges and co-sediments with lithogenic material if present. The POM: dw ratio during bloom events was 23%, and thus very similar to non-bloom conditions. Bloom and non-bloom intervals were categorized by POM sedimentation rates greater or less than 150 mg m^{-2} d^{-1}, respectively.

3.2. Laboratory experiments

3.2.1. Formation of macroaggregates from resuspended sediments

Bottom water and resuspended sediments (BW+seds) formed macroaggregates > 1 mm in diameter within the first day of the roller bottle experiment (approximately 200 aggregates L^{-1}; see Suppl. Fig. S4 for pictures of the roller bottle). Aggregate sizes and numbers appeared to be unchanged until the end of the incubation at day 7 (based on qualitative observations of roller bottle aggregates). Visible aggregates did not form in either of the roller bottles with live (BW) or with autoclaved control bottom water (BW control) that lacked sediments.

3.2.2. Bacterial activities and abundances

Initial bacterial cell abundance in BW+seds was a factor of ca. 2.5 higher compared to the roller bottle with unamended bottom water (BW) (Table 4). Initial BW cell numbers were the same order of magnitude as those in OC26 bottom waters (Table 2); thus storage of experimental bottom waters until the beginning of the roller bottle experiment had little effect on cell numbers. At day 4, cell abundances in both bottles were approximately double their initial values; at day 7, bacterial abundances in the presence and absence of resuspended sediments decreased back to initial levels.

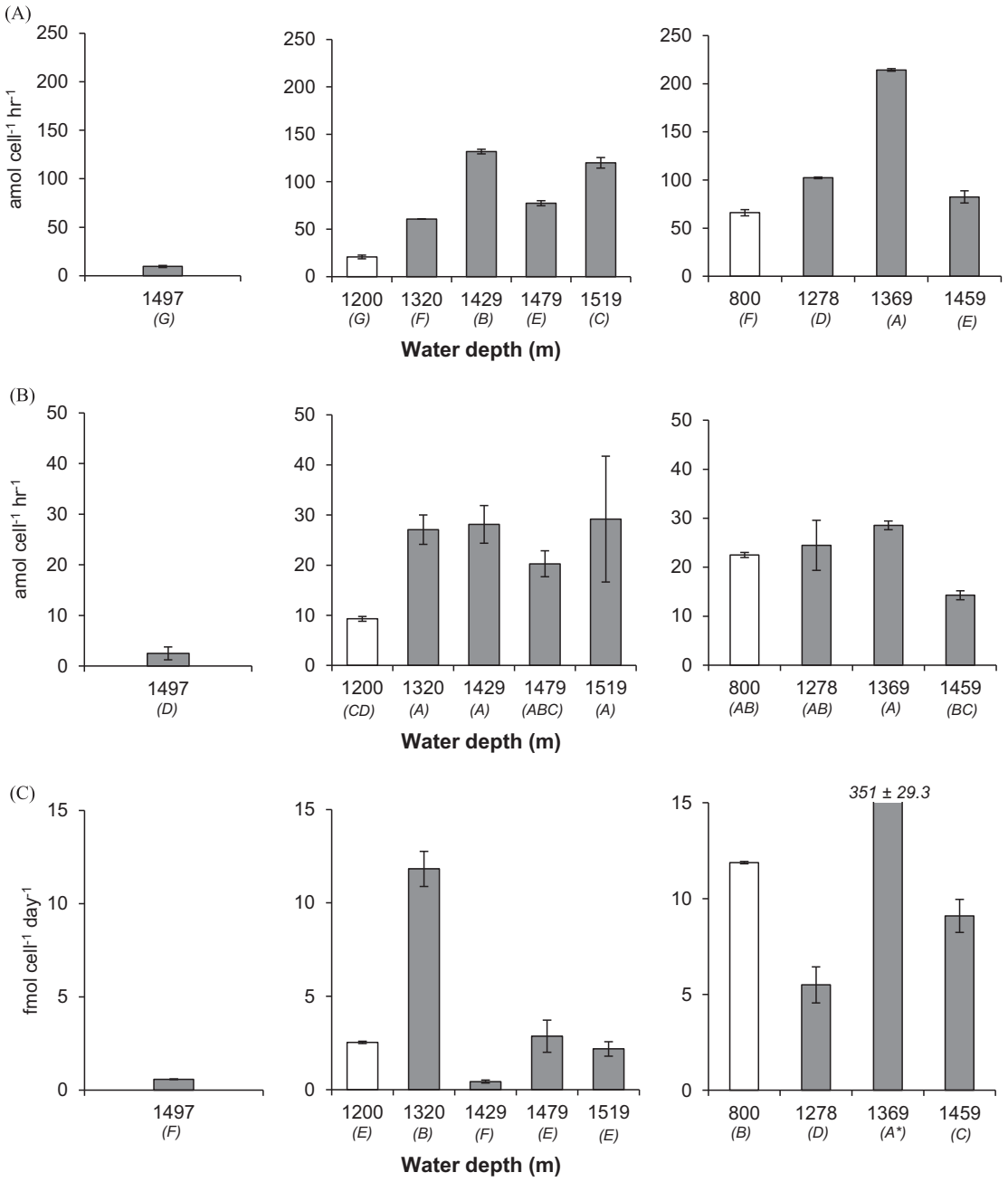

Fig. 4. Bacterial activities in bottom waters of casts 1 (left panels), 2 (middle panels), and 7 (right panels). Cell-specific peptidase (A), cell-specific β-glucosidase (B), cell-specific leucine incorporation (C) within the BNL (gray bars) and above the BNL (white bars). Letters in parenthesis indicate the results of the post-hoc analysis of depth-specific differences in rates ($p < 0.05$); rates with the same letters are indistinguishable from one another.

Increases in enzyme activities over the time course of roller bottle incubation far outpaced increases in bacterial numbers. On a volume basis, peptidase and β-glucosidase activities increased by a factor of six between day 0 and day 4 (BW+seds) and by a factor of ten for BW β-glucosidase (Table 4). At day 7, enzyme activities were lower than at day 4, but were still approximately a factor of three higher than at day 0. On a cell-specific basis, peptidase as well as β-glucosidase activities increased by a factor of three to five between day 0 and day 4. For BW+seds, enzyme activities at day 7 were comparable to day 4. For the BW bottle, only cell-specific β-glucosidase activities at day 7 were comparable to day 4. At day 7, cell specific peptidase activities for the BW bottle were still a factor of 2.5 higher than at day 0 (Table 4). Peptidase and β-glucosidase activities on a volume and on a cell-specific basis were always higher in BW+seds compared to BW (Table 4), with the exception of cell-specific peptidase activities at day 4, which were similar in both roller bottles (Table 4).

Changes in leucine incorporation did not outpace changes in cell numbers in the BW+seds bottle. Bulk rates of leucine incorporation increased by only 20% by day 4, and decreased to ca. half of initial levels by day 7. In the BW bottles, however, bulk leucine incorporation increased by a factor of ca. 80 between 0 and 4 days, outpacing increases in cell numbers. At day 7, leucine incorporation was still a factor of 20 higher than at day 0. On a cell-specific level, leucine incorporation increased sharply in the BW bottle, but decreased in the BW+seds bottle. Although cell-specific leucine incorporation was initially higher in the BW+seds bottle, at days 4 and 10, cell-specific leucine incorporation was much higher in the BW bottle than in the BW+seds bottle (Table 4).

3.2.3. Polysaccharide hydrolysis after the roller bottle incubation

The polysaccharide hydrolysis experiment initiated at the conclusion of the roller bottle incubation revealed a broader enzymatic spectrum and generally higher hydrolysis rates in BW+seds compared to BW (Table 5). Most notably, only three of the six polysaccharides (laminarin, xylan, chondroitin) were hydrolyzed in BW, whereas four substrates (laminarin, xylan, chondroitin, pullulan) were hydrolyzed in BW+seds. For all substrates, hydrolysis was more rapid in BW+seds compared to BW incubations.

Hydrolysis rates and patterns differed substantially among substrates. For example, pullulan hydrolysis was detectable comparatively late in the BW+seds incubations (only starting at day 7), and at rates an order of magnitude lower compared to the other three substrates that were hydrolyzed (Table 5). Laminarin hydrolysis, in contrast, was comparatively rapid and at maximum rates at day 3 in BW as well as in BW + seds. Xylan hydrolysis was maximal at day 7 in BW+seds, and at day 14 in BW, whereas chondroitin hydrolysis rates were highest at day 7 in BW as well as in BW + seds. Neither arabinogalactan nor fucoidan were hydrolyzed in any of the incubations (Table 5).

Bacterial cell numbers varied for the most part between 10 and 20×10^7 cells L^{-1} during the 22-day polysaccharide hydrolysis experiment (Table 5). No notable differences in cell numbers were observed between the vials in which hydrolysis was detected compared to those without measurable hydrolysis (Table 5). Cell numbers in the vials that had no polysaccharide substrate added were in the same range as those with added substrates, indicating that polysaccharide additions did not notably enhance net cell growth. Leucine incorporation rates were generally higher in BW compared to BW+seds, following the pattern observed during the roller bottle incubation (Table 4). Leucine incorporation rates were for the most part highest in the beginning of the experiment, and in all cases decreased over time.

Table 3
POM and lithogenic particles sedimentation rates (mg m^{-2} d^{-1}) and the POM: dw ratios during sedimenting phytoplankton blooms (Bloom) and non-bloom conditions from January 2011 until September 2013 (median rates; 1st, 3rd quartile in brackets) as well as during the BNL event (Aug 12, 2012–Sept 8, 2012); *n* is the number of collection cups.

Sample type	POM (mg m^{-2} d^{-1})	Lithogenic	POM: DW
Non-bloom ($n=30$)	58 (43–84)	161 (117–239)	25%
Bloom ($n=7$)	187 (170–206)	494 (473–606)	23%
BNL ($n=1$)[a]	79	426	13%

[a] data confirmed by deep trap which shows the same abnormality

4. Discussion

A thick bottom nepheloid layer (BNL) was detected in the deep Mississippi Canyon in the area of station OC26 over at least 3.5 km^2 throughout the 9-day survey. We hypothesize that this BNL formed as a result of Hurricane Isaac, which passed over the study area and made landfall on the Louisiana coast one week before the start of our sampling campaign (Berg, 2013). The sediment trap time series showed exceptionally high sedimentation of lithogenic material in the absence of organic carbon in late August/early September 2012 (Table 3), suggesting a lateral transport of resuspended sediments from the shelf into our investigation area. Previous studies documented the effects of passing hurricanes on water circulation and current patterns (Brooks, 1983; Keen and Allen, 2000; Shay and Elsberry, 1987) as well as sediment resuspension on the Louisiana shelf (Ross et al. 2009). For example, in the aftermath of Hurricane George in 1998, down-canyon transport of resuspended sediments into the Mississippi Canyon continued for days to weeks after the storm had passed (Ross et al. 2009). Following Hurricane Ivan in 2004, Bianchi et al. (2006) found surficial sediment layers of terrigenous material with a riverine isotopic signal in the Mississippi Canyon. High Mississippi River discharge can initiate down-canyon transport of BNLs as riverine particles in the river plumes at the surface undergo rapid coagulation and sinking processes, forming easily resuspendable sediment layers on the shelf (Ross et al. 2009). A relationship between Mississippi River discharge and the presence of BNLs in the Mississippi Canyon throughout our investigation period (i.e. up to two weeks after the hurricane made landfall) is plausible; Mississippi River runoff likely continued for up to 10 days, considering a storm surge of 300 river miles followed by an

Table 4
Bacterial cells ($\times 10^7$ L^{-1}), peptidase and β-glucosidase activity (pM h^{-1}), cell-specific peptidase and glucosidase activity (amol $cell^{-1}$ h^{-1}), leucine incorporation (leu incorp; pM h^{-1}), cell-specific leucine incorporation (amol $cell^{-1}$ day^{-1}) throughout the 7-days roller bottle experiment. BW+seds: bottom water with resuspended sediments; BW: bottom water lacking resuspended sediments. *P*-values are from Student's t-test. Letters indicate results of post hoc analysis of timepoint-specific differences of bacterial activities ($p < 0.05$). Rates with the same letters are indistinguishable from one another; n.s. means not significant.

		Day 0	Day 4	Day 7
Cells	BW+seds	20	48.5	22.9
	BW	7.5	15.6	8.9
Peptidase	BW+seds	2513 ± 67; C	17310 ± 8.4; A	8745 ± 335; B
	BW	620 ± 12; C	6088 ± 402; A	1876 ± 154; B
	P	*1.3E-03*	*3.1E-0.5*	*5.5E-06*
Cell-specific peptidase	BW+seds	12.5 ± 0.3; B	35.7 ± 1.7; A	38.2 ± 1.5; A
	BW	8.3 ± 0.2; C	39 ± 2.6; A	21.2 ± 1.7; B
	P	*7.4E-03*	*n.s.*	*2.1E-04*
β-glucosidase	BW+seds	1070 ± 18; C	7268 ± 568; A	3289 ± 265; B
	BW	111 ± 49; B	1291 ± 102; A	607 ± 274; B
	P	*1.5E-03*	*6.5E-05*	*2.6E-04*
Cell-specific β-glucosidase	BW+seds	5.3 ± 0.1; B	15 ± 1.2; A	14.4 ± 1.2; A
	BW	1.5 ± 0.7; B	8.3 ± 0.7; A	6.9 ± 3.1; AB
	P	*1.4E-02*	*1.1E-03*	*1.7E-02*
Leu incorp	BW+seds	63.4 ± 8.3; A	74.5 ± 4.2; A	35.2 ± 5; B
	BW	1.6 ± 0.3; C	115 ± 9.8; A	39.2 ± 6.7; B
	P	*2.1E-04*	*2.7E-03*	*n.s.*
Cell-specific leu incorp	BW+seds	7.6 ± 1; A	3.7 ± 0.2; B	3.7 ± 0.5; B
	BW	0.5 ± 0.1; C	17.7 ± 1.5; A	10.6 ± 1.8; B
	P	*2.6E-04*	*9.1E-05*	*3.2E-03*

Table 5
Results of polysaccharide hydrolysis experiment following the 7-days roller bottle incubation. Bacterial cells ($\times 10^7$ L^{-1}), polysaccharide hydrolysis rates (Hdr; nM monomer h^{-1}), and leucine incorporation rates (leu incorp; pM h^{-1}); BW+seds: bottom water with resuspended sediments; BW: bottom water lacking resuspended sediments. Letters indicate results of post hoc analysis of timepoint-specific differences of bacterial activities ($p < 0.05$). Rates with the same letters are indistinguishable from one another; n.d. means not determined.

			Day 3	Day 7	Day 14	Day 22
Pullulan	BW+seds	Hdr	0; B	0.3 ± 0.1; A	0.4 ± 0.0*; A	0.4 ± 0.1; A
		Leu incorp	80.9 ± 0.5; A	69.1 ± 4.1; A	21.2 ± 2.4; B	24 ± 1; B
		Cells	32.2	14.9	14.5	11.2
	BW	Hdr	0	0	0	0
		Leu incorp	128 ± 0.5; A	108 ± 3.9; B	108 ± 9.4; B	88.6 ± 10.8; C
		Cells	16.7	9	13.5	21.9
Laminarin	BW+seds	Hdr	16.9 ± 1; A	11.2 ± 0.1; B	6.5 ± 0.1; C	4.4 ± 0.0*; C
		Leu incorp	92.5 ± 11.2; A	67.2 ± 0.3; A	17.9 ± 0.6; B	15.8 ± 0.4; B
		Cells	18.7	11.3	10.2	11.9
	BW	Hdr	12.1 ± 0.5; A	9.9 ± 0.5; B	5.4 ± 0.2; C	4 ± 0.0*; C
		Leu incorp	121.5 ± 4.9; A	97.6 ± 6.7; B	58.3 ± 3.8; C	95.2 ± 4.4; B
		Cells	32.2	10.7	17.1	20
Xylan	BW+seds	Hdr	3.4 ± 0.4; D	13.5 ± 0.1; A	7 ± 0.0*; B	4.6 ± 0.0*; C
		Leu incorp	71.2 ± 3.9; A	37.1 ± 1.1; B	27.2 ± 2.6; BC	23 ± 0.2; C
		Cells	15.7	9.3	21.4	11.2
	BW	Hdr	0; D	2.1 ± 0.1; C	6.1 ± 0.0*; A	4.1 ± 0.0*; D
		Leu incorp	89.5 ± 10.7; A	85.3 ± 4.8; AB	19.0 ± 0.5; C	30.1 ± 18.2; BC
		Cells	18.3	13.1	15.1	25.5
Chondroitin	BW+seds	Hdr	11.0 ± 0.6; B	16.9 ± 0.3; A	9 ± 0.1; C	5.8 ± 0.0*; D
		Leu incorp	79.4 ± 5.7; A	43.5 ± 7; B	45.3 ± 0.6; B	27.5 ± 0.0*; B
		Cells	16.8	8.9	n.a.	14.5
	BW	Hdr	7.8 ± 0.6; B	15.5 ± 0.0*; A	7.8 ± 0.1; B	5.1 ± 0.1; C
		Leu incorp	104.2 ± 1.2; A	68.8 ± 0.8; B	54.2 ± 4.7; C	25.7 ± 0.0*; D
		Cells	17.5	11.5	n.d.	13.8
Arabinogalactan	BW+seds	Hdr	0	0	0	0
		Leu incorp	70.7 ± 5.2; A	41.6 ± 1.6; B	13.3 ± 5.8; C	12.4 ± 1.5; C
		Cells	10.1	23.8	n.d.	18.6
	BW	Hdr	0	0	0	0
		Leu incorp	113.8 ± 0.9; A	96.5 ± 8.9; A	44.0 ± 4.9; B	60.7 ± 3.3; B
		Cells	11	16.7	11.5	14.1
Fucoidan	BW+seds	Hdr	0	0	0	0
		Leu incorp	58.5 ± 3.0; A	54.2 ± 0.6; AB	21.4 ± 1.3; BC	10.6 ± 1.1; C
		Cells	10.4	11.4	7.3	15.3
	BW	Hdr	0	0	0	0
		Leu incorp	105.6 ± 1.4; A	90.3 ± 1; B	30.2 ± 3.4; D	44.7 ± 3.7; C
		Cells	14.4	18.7	14.3	12.9
No substrate	BW+seds	Hdr	–	–	–	–
		Leu incorp	47.5 ± 6.3; A	50.7 ± 1; A	17.5 ± 1.3; B	12.9 ± 1; B
		Cells	10.1	9.6	6.7	15.4
	BW	Hdr	–	–	–	–
		Leu incorp	122 ± 5.7; A	96.5 ± 3.2; B	32.0 ± 1.8; C	32.3 ± 1.8; C
		Cells	11	12.3	n.d.	12.4

* error < 0.05

average downstream river flow of 50 cm s^{-1} (US Army Corps of Engineers, 2013). Downslope transport of BNLs from the shelf into the investigation area (distance ~80 km) would have required an additional 10 days, based on average bottom water currents of 8 cm s^{-1} measured earlier at a nearby site during non-storm conditions (Ross et al., 2009).

Peak velocities of down-canyon turbidity currents during our investigation period likely exceeded 8 cm s^{-1}, based on previous observations. In the aftermath of Hurricane George in 1998, for example, maximum near-bed flow velocities in the Mississippi Canyon reached 60 cm s^{-1}, triggering resuspension of local sediments up to 50 m above the seafloor (Ross et al., 2009). Resuspension heights in deep sea environments may at times extend to about 100 m above the sea floor (Gardner et al., 1983); we therefore assume that the lower part of the BNL at OC26 below the turbidity front was a mixture of locally resuspended sediments and sediment suspensions that were transported laterally into the study area. Sediment resuspension often carries inorganic nutrients and particulate organic matter into the overlying water column Chrost, Rieman (1994). We found evidence for relatively fresh organic matter (low C/N ratios) associated with the BNL (casts 1 and 7; Table 2) with POC concentrations that were up to one order of magnitude higher than those reported in a previous study from the same area in the Gulf of Mexico (Cherrier et al., 2014).

Enhanced fluxes of (re-)suspended sediments stimulated heterotrophic bacterial enzymatic activities in the BNL, especially in locations where the turbidity transition was most pronounced (casts 2 and 7; Fig. 4; Table 2), to levels that exceeded those in the overlying water column. Maximum bottom water peptidase and β-glucosidase activities were also higher compared to deep water rates from other deep-ocean regions (Baltar et al., 2009; 2010; Hoppe and Ullrich, 1999). Compared to our previous study in the same region of the Gulf of Mexico (Ziervogel and Arnosti, 2013), highest cell-specific activities within the BNL were similar (peptidase) and more than a factor of 30 higher (β-glucosidase). Despite our observation of generally enhanced enzymatic activities within the BNL, we also found substantial spatial differences in bacterial activities and abundance among the three bottom water CTD casts (Fig. 4; Table 2). These variations are likely the result of the spatial and temporal heterogeneity of the BNL (Fig. 1) caused in part by bottom topography. The differences in the turbidity profiles of the six casts (Fig. 2) further support this hypothesis.

The presence of resuspended sediments in bottom waters stimulates microbial enzyme activities, as demonstrated by our roller bottle experiment as well as our field observations. Bacterial cell numbers prior to the start of the laboratory incubation reveal that the resuspended sediment slurry (BW+seds) was densely populated by bacterial cells that likely contributed a substantial fraction of overall bacterial activities throughout the incubation. Bacteria associated with surficial sediments and other marine particles often show higher enzymatic activities, as well as a broader range of enzymes compared to those in the overlying water column (Arnosti, 1998; 2000; 2008; Arnosti et al., 2009; Hoppe et al., 2002; Teske et al., 2011; Ziervogel and Arnosti, 2009), likely due to the fact that sedimentary bacteria are exposed to a broader range of organic substrates compared to pelagic bacteria.

The importance of particle-associated bacteria in the BW+seds roller bottle is also supported by our observation of a broader range of polysaccharide hydrolases in the presence of resuspended sediments compared to the unamended bottom water (Table 5). Our previous investigations of microbial enzyme activities in the deep Mississippi Canyon area using the same suite of polysaccharide substrates also demonstrated that only laminarin, xylan, and chondroitin were hydrolyzed (Steen et al., 2012; Ziervogel and Arnosti, 2013), the same pattern seen in the BW incubations in the present study. The fact that pullulan hydrolysis was measurable in the BW+seds bottle points to a metabolic capability common among benthic and particle-associated bacterial communities, but comparatively rare in the open ocean (Arnosti (2011) and references therein).

Leucine incorporation rates, as a measure of bacterial protein production and thus overall community activities, were generally lower in BW+seds compared to the BW during the roller bottle experiment, despite the substantially higher hydrolytic activities in the BW+seds (Table 4). Potentially, benthic bacteria may have a greater number of (or more highly active) enzymes ready to hydrolyze any potential substrates compared to their pelagic counterparts. Alternatively, a fraction of extracellular enzymes may have already been present in the sediments, adsorbed to particles, at the start of the incubation. Heterotrophic bacteria in marine sediments and other particle-rich environments release high levels of extracellular enzymes into their environment where they adsorb to particles, thus remaining in relatively close contact to the cells that produced them (Vetter et al., 1998). Particle-attached cell-free enzymes have been shown to retain their hydrolytic activities over time courses longer than our 7-days roller bottle incubation (Steen and Arnosti, 2011; Ziervogel et al., 2011).

Our roller bottle experiment further demonstrated that resuspended sediments from the investigation area undergo rapid coagulation, resulting in the formation of macroaggregates. The first marine snow camera cast (cast 3; Fig. 3) also showed elevated numbers of macroaggregates near the seafloor compared to the later casts, casts 6 and 9. This difference in contribution of larger aggregates to total aggregates may have resulted from aggregation of resuspended OC26 sediments. A nearby origin of these larger aggregates is implied by the fact that macroaggegates in bottom waters are subject to sinking and re-deposition on the seafloor (Thomsen and McCave, 2000). We calculated maximum residence times for aggregated resuspended sediments in the BNL on the order of 3 days, assuming a resuspension height of 100 m and aggregate sinking velocities of 34 m d^{-1}. This sinking velocity is based on in situ sinking velocities of aggregates in the mid-water column, measured at a nearby site (Diercks and Asper, 1997). A residence time of 3 days is in the same range as the incubation intervals of roller bottle aggregates before and after the first sampling. During this time, bacteria associated with aggregates of resuspended sediments may have respired and considerably transformed fractions of sedimentary particulate matter.

Resuspension events of OC26 sediments like the one we observed in the aftermath of Hurricane Isaac may periodically transport sedimented organic matter into the overlying water where it enters microbial food webs. Such event-driven resuspension events in our investigation area could have led to the redistribution of sedimented oil-fallout and associated substances (e.g. chemical dispersants) in the aftermath of the Deepwater Horizon oil spill in 2010, affecting bottom water carbon cycling in the deep Gulf of Mexico.

Acknowledgments

We thank the captains and shipboard parties of the R/V *Endeavor* (cruise 515) and the R/V *Falkor* (cruise FK0066). We thank Dr. Andrew Juhl (LDEO, Columbia University) for the use of equipment and supplies for microscopy, and Kendra Bullock (Columbia University), for assistance with microscopy. Julia Sweet (University of California, Santa Barbara) helped sampling as well as processing and analyzing the sediment trap samples. This research was supported by a grant from BP/the Gulf of Mexico Research Initiative to support consortium research entitled “Ecosystem Impacts of Oil and Gas Inputs to the Gulf (ECOGIG)”. This is ECOGIG contribution # 358 and the data are archived at GRIIDC under UDI# R1.x132.134:0080.

Appendix A. Supporting information

Supplementary data associated with this article can be found in the online version at http://dx.doi.org/10.1016/j.dsr2.2015.06.017.

References

Alderkamp, A.C., van Rijssel, M., Bolhuis, H., 2007. Characterization of marine bacteria and the activity of their enzyme systems involved in degradation of the algal storage glucan laminarin. FEMS Microbiol. Ecol. 59, 108–117.
Aristegui, J., Gasol, J.M., Duarte, C.M., Herndl, G.J., 2009. Microbial oceanography of the dark ocean's pelagic realm. Limnol. Oceanogr. 54, 1501–1529.
Arnosti, C., 2011. Microbial extracellular enzymes and the marine carbon cycle. Ann. Rev. Mar. Sci. 3, 401–425.
Arnosti, C., 2008. Functional differences between arctic sedimentary and seawater microbial communities: contrasts in microbial hydrolysis of complex substrates. FEMS Microbiol. Ecol. 66, 343–351.
Arnosti, C., 2003. Fluorescent derivatization of polysaccharides and carbohydrate-containing biopolymers for measurement of enzyme activities in complex media. J. Chromatogr. B 793, 181–191.
Arnosti, C., 2000. Substrate specificity in polysaccharide hydrolysis: contrasts between bottom water and sediments. Limnol. Oceanogr. 45, 1112–1119.
Arnosti, C., 1998. Rapid potential rates of extracellular enzymatic hydrolysis in arctic sediments. Limnol. Oceanogr. 43, 315–324.
Arnosti, C., Ziervogel, K., Ocampo, L., Ghobrial, S., 2009. Enzyme activities in the water column and in shallow permeable sediments from the northeastern Gulf of Mexico. Est. Coast. Shelf Sci 84, 202–208.
Atlas, R.M., Hazen, T.C., 2011. Oil biodegradation and bioremediation: a tale of the two worst spills in US history. Environ. Sci. Technol. 45, 6709–6715.
Baltar, F., Aristegui, J., Gasol, J.M., Sintes, E., van Aken, H.M., Herndl, G.J., 2010. High dissolved extracellular enzymatic activity in the deep central Atlantic Ocean. Aquat. Microbiol. Ecol. 58, 287–302.
Baltar, F., Aristegui, J., Sintes, E., van Aken, H.M., Gasol, J.M., Herndl, G.J., 2009. Prokaryotic extracellular enzymatic activity in relation to biomass production and respiration in the meso- and bathypelagic waters of the (sub)tropical Atlantic. Environ. Microbiol. 11, 1998–2014.
Berg, R., 2013. Hurricane Isaac tropical cyclone report. National Hurricane Center, 1–78.
Bianchi, T.S., Allison, M.A., Canuel, E.A., Corbett, D.R., McKee, B.A., Sampere, T.P., Makeham, S.G., Waterson, E., 2006. Rapid export of organic matter to the Mississippi Canyon. Eos 87 (565), 572–573.
Boetius, A., Springer, B., Petry, C., 2000. Microbial activity and particulate matter in the benthic nepheloid layer (BNL) of the deep Arabian Sea. Deep-Sea Res. II 47, 2687–2706.
Brooks, D.A., 1983. The wake of Hurricane Allen in the western Gulf of Mexico. J. Phys. Oceanogr. 13, 117–129.
Cherrier, J., Sarkodee-Adoo, J., Guilderson, T.P., Chanton, J.P., 2014. Fossil carbon in particulate organic matter in the Gulf of Mexico following the Deepwater Horizon event. Environ. Sci. Technol. Lett 1, 108–112.

Chrost, R.J., Rieman, B., 1994. Storm-stimulated enzymatic decomposition of organic matter in benthic/pelagic coastal mesocosms. Mar. Ecol. Prog. Ser. 108, 185–192.
DeMaster, D., 1981. The supply and accumulation of silica in the marine environment. Geochim. Cosmochim. Acta 45, 1715–1732.
Diercks, A.R., Asper, V.L., 1997. In situ settling speeds of marine snow aggregates below the mixed layer: Black Sea and Gulf of Mexico. Deep-Sea Res. I 44, 385–398.
Fohrmann, H., Backhaus, J., Blaume, F., Rumohr, J., 1998. Sediments in bottom-arrested gravity plumes: numerical case studies. J. Phys. Oceanogr. 28, 2250–2274.
Gardner, W., Richardson, M., Hinga, K., Biscaye, P., 1983. Resuspension measured with sediment traps in a high-energy environment. Earth Planet Sci. Lett. 66, 262–278.
Graf, G., Rosenberg, R., 1997. Bioresuspension and biodeposition: a review. J. Mar. Sys 11, 269–278.
Hollister, C., McCave, I., 1984. Sedimentation under deep-sea storms. Nature 309, 220–225.
Hoppe, H.G., 1983. Significance of exoenzymatic activities in the ecology of brackish water - measurements by means of methylumbelliferyl-substrates. Mar. Ecol. Prog. Ser. 11, 299–308.
Hoppe, H.G., Ullrich, S., 1999. Profiles of ectoenzymes in the Indian Ocean: phenomena of phosphatase activity in the mesopelagic zone. Aquat. Microb. Ecol. 19, 139–148.
Hoppe, H.G., Arnosti, C., Herndl, G.J., 2002. Ecological significance of bacterial enzymes in the marine environment. In: Burns, R.G., Dick, R.P. (Eds.), Enzymes in the Environment. Marcel Dekker, New York, pp. 73–108.
Kirchman, D.L., 2001. Measuring bacterial biomass production and growth rates from leucine incorporation from aquatic environments. In: Paul, J.H. (Ed.), Marine Microbiology – Methods in Microbiology. Academic Press, pp. 227–237.
Keen, T.R., Allen, S.E., 2000. The generation of internal waves on the continental shelf by Hurricane Andrew. J. Geophys. Res. 105, 26203–26224.
Lunau, M., Lemke, A., Walther, K., Martens-Habbena, W., Simon, M., 2005. An improved method for counting bacteria from sediments and turbid environments by epifluorescence microscopy. Environ. Microbiol. 7, 961–968.
McCave, I., 1986. Local and global aspects of the bottom nepheloid layers in the world ocean. J. Sea Res. 20, 167–181.
Mortlock, R.A., Froelich, P.N., 1989. A simple method for the rapid determination of biogenic opal in pelagic marine sediments. Deep-Sea Res I 36, 1415–1426.
Painter, T.J., 1983. Algal polysaccharides. In: Aspinall, G.O. (Ed.), The Polysaccharides. Academic Press, New York, pp. 195–285.
Porter, K.G., Feig, Y.S., 1980. The use of DAPI for identifying and counting aquatic microflora. Limnol. Oceanogr. 25, 943–948.
Puig, P., Ogston, A., Mullenbach, B., Nittrouer, C., Parsons, J., Sternberg, R., 2004. Storm-induced sediment gravity flows at the head of the eel submarine canyon, northern California margin. J. Geophys. Res. 109, C03019.
Puig, P., de Madron, X.D., Salat, J., Schroeder, K., Martin, J., Karageorgis, A.P., Palanques, A., Roullier, F., Luis Lopez-Jurado, J, Emelianov, M, Moutin, T., Houpert, L., 2013. Thick bottom nepheloid layers in the western Mediterranean generated by deep dense shelf water cascading. Prog. Oceanogr. 111, 1–23.
Ritzrau, W., Graf, G., 1992. Increase of microbial biomass in the benthic turbidity zone of Kiel Bight after resuspension by a storm event. Limnol. Oceanogr. 37, 1081–1086.
Ritzrau, W., Thomsen, L., Lara, R., Graf, G., 1997. Enhanced microbial utilisation of dissolved amino acids indicates rapid modification of organic matter in the benthic boundary layer. Mar. Ecol. Prog. Ser. 156, 43–50.
Ross, C.B., Gardner, W.D., Richardson, M.J., Asper, V.L., 2009. Currents and sediment transport in the Mississippi Canyon and effects of Hurricane Georges. Cont. Shelf Res. 29, 1384–1396.
Shay, L.K., Elsberry, R.L., 1987. Near-internal ocean current response to Hurricane Frederic. J. Phys. Oceanogr. 17, 1249–1269.
Shipe, R.F., Brzezinski, M.A., 2003. Siliceous plankton dominate primary and new productivity during the onset of El Nino conditions in the Santa Barbara Basin, California. J. Marine Syst. 42, 127–143.
Steen, A.D., Arnosti, C., 2011. Long lifetimes of beta-glucosidase, leucine aminopeptidase, and phosphatase in arctic seawater. Mar. Chem. 123, 127–132.
Steen, A.D., Ziervogel, K., Ghobrial, S., Arnosti, C., 2012. Functional variation among polysaccharide-hydrolyzing microbial communities in the Gulf of Mexico. Mar. Chem. 138, 13–20.
Stevens, H., Brinkhoff, T., Simon, M., 2005. Composition of free-living, aggregate-associated and sediment surface-associated bacterial communities in the German Wadden Sea. Aquat. Microb. Ecol. 38, 15–30.
Teske, A., Durbin, A., Ziervogel, K., Cox, C., Arnosti, C., 2011. Microbial community composition and function in permanently cold seawater and sediments from an arctic fjord of Svalbard. Appl. Environ. Microbiol. 77, 2008–2018.
Thomsen, L., 1999. Processes in the benthic boundary layer at continental margins and their implication for the benthic carbon cycle. J. Sea Res. 41, 73–86.
Thomsen, L., Graf, G., 1994. Characteristics of suspended particulate matter in the benthic boundary layer of the continental margin of the Western Barents Sea. Oceanol. Acta 17, 597–607.
Thomsen, L., McCave, I., 2000. Aggregation processes in the benthic boundary layer at the Celtic Sea continental margin. Deep-Sea Res I 47, 1389–1404.
Turley, C., 2000. Bacteria in the cold deep-sea benthic boundary layer and sediment-water interface of the NE Atlantic. FEMS Microbiol. Ecol. 33, 89–99.
US Army Corps of Engineers, 2013. Hurricane Isaac with and without 2012 100-year HSDRRS evaluation. Final Report. pp. 230.
Vetter, Y.A., Deming, J.W., Jumars, P.A., Kreiger-Brockett, B.B., 1998. A predictive model of bacterial foraging by means of freely released extracellular enzymes. Microb. Ecol. 36, 75–92.
Ziervogel, K., Steen, A.D., Arnosti, C., 2011. Changes in the spectrum and rates of extracellular enzyme activities in seawater following aggregate formation. Biogeosciences 7, 1007–1015.
Ziervogel, K., McKay, L., Rhodes, B., Osburn, C.L., Dickson-Brown, J., Arnosti, C., Teske, A., 2012. Microbial activities and dissolved organic matter dynamics in oil-contaminated surface seawater from the Deepwater Horizon oil spill site. PLoS One 7, e34816.
Ziervogel, K., Arnosti, C., 2009. Enzyme activities in the Delaware Estuary affected by elevated suspended sediment load. Est. Coast. Shelf Sci. 84, 253–258.
Ziervogel, K., Arnosti, C., 2013. Enhanced protein and carbohydrate hydrolyses in plume-associated deepwaters initially sampled during the early stages of the Deepwater Horizon oil spill. Deep-Sea Res II: http://dx.doi.org/10.1016/j.dsr2.2013.09.003i.